



Review

# Acetylene polymerization on supported transition metal clusters

Ken Judai<sup>a</sup>, Stéphane Abbet<sup>a</sup>, Anke S. Wörz<sup>a</sup>, Anna Maria Ferrari<sup>b</sup>,  
Livia Giordano<sup>c</sup>, Gianfranco Pacchioni<sup>c</sup>, Ueli Heiz<sup>a,\*</sup>

<sup>a</sup> *Institute of Surface Chemistry and Catalysis, University of Ulm, D-89069 Ulm, Germany*

<sup>b</sup> *Dipartimento di Chimica IFM, Università di Torino, I-10125 Torino, Italy*

<sup>c</sup> *Dipartimento di Scienza dei Materiali, Istituto Nazionale per la Fisica della Materia,  
Università di Milano-Bicocca, I-20125 Milano, Italy*

Received 15 April 2002; received in revised form 2 July 2002; accepted 2 July 2002

## Abstract

The polymerization of acetylene, studied experimentally and theoretically on nanocatalysts consisting of nanoscale clusters of different size and elemental composition, is reviewed. As on bulk systems palladium is the most active transition metal for this reaction. More important, however, is the changing selectivity as function of size and elemental composition. As an example, palladium atoms, dimers, and trimers, as well as nanoscale copper clusters are highly selective for the cyclotrimerization reaction. In the case of palladium, the  $\pi$ -bonding of acetylene and a charge transfer from the substrate to the atom/cluster are responsible for the high selectivity. In addition DFT calculations revealed the whole reaction path of this reaction on palladium atoms and it could be shown that in contrast to bulk systems the rate-determining step is the formation of benzene from the  $\text{Pd}(\text{C}_4\text{H}_4)\text{C}_2\text{H}_2$  complex.

© 2003 Elsevier Science B.V. All rights reserved.

**Keywords:** Nanocatalysis; Cyclotrimerization; Polymerization; Clusters; Selectivity

## 1. Introduction

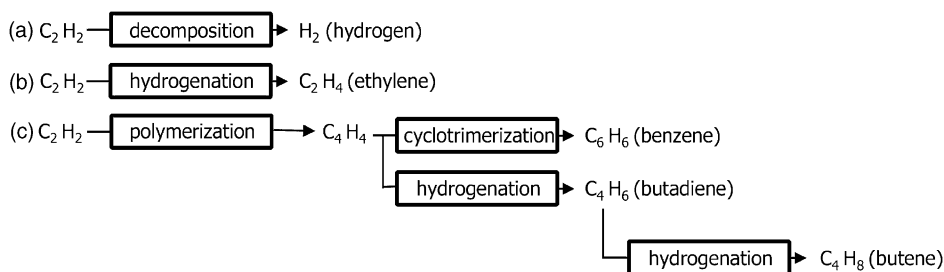
The acetylene ( $\text{C}_2\text{H}_2$ ) polymerization is one of the possible observed reaction paths when acetylene is catalytically transformed. First, the acetylene molecule can decompose to produce hydrogen ( $\text{H}_2$ ) and residual hydrocarbons or carbon (Scheme 1a). Second, the hydrogenation of acetylene results in the production of ethylene ( $\text{C}_2\text{H}_4$ ) (Scheme 1b). Finally, during the polymerization, the  $\text{C}_4\text{H}_4$  intermediate is formed (Scheme 1c), resulting from the combination of two acetylene molecules. Addition of a third activated acetylene molecule may then lead to the forma-

tion of benzene ( $\text{C}_6\text{H}_6$ ). This polymerization reaction is called the cyclotrimerization. In a parallel reaction, the hydrogenation of the intermediate may also be catalyzed to produce butadiene ( $\text{C}_4\text{H}_6$ ). Sequentially, the hydrogenation of butadiene results in the production of butene ( $\text{C}_4\text{H}_8$ ). Thus, the polymerization of acetylene may result in three possible, different product molecules: benzene, butene and butadiene.

On single palladium crystals acetylene is decomposed or polymerized [1]. For the latter reaction path only the cyclotrimerization is observed and  $\text{Pd}(111)$  is found to be the most reactive facet [1–3]. At high coverage or pronounced surface roughness, the formed benzene is forced into a weaker binding configuration with the molecular axis tilted with respect to the surface. From this tilted configuration, benzene desorbs

\* Corresponding author.

E-mail address: [ulrich.heiz@chemie.uni-ulm.de](mailto:ulrich.heiz@chemie.uni-ulm.de) (U. Heiz).



Scheme 1. Different observed reactions of adsorbed acetylene on pure [1,3,4] and mixed palladium catalysts [13,14,47]. (a) Decomposition of  $C_2H_2$  and formation of  $H_2$ ; (b) hydrogenation of  $C_2H_2$  with the formation of ethylene; (c) polymerization of  $C_2H_2$  and the formation of benzene, butadiene or butene.

already at a temperature of 230 K. At low coverage and on flat surfaces the formed  $C_6H_6$  binds strongly to the surface in a flat-lying configuration and desorbing at a temperature of  $\sim 500$  K [4–6]. It is believed that the reaction takes place without C–C bond scission [7], and it appears that in a first step acetylene is adsorbed in the three-fold hollow site on palladium [8,9] via two  $\sigma$ -bonds and a  $\pi$ -bond (di- $\sigma/\pi$  configuration). This configuration leads to adsorbed  $C_2H_2$  in a flat-lying geometry and the electronic structure is grossly distorted from  $sp^1$  to  $sp^{2.5}$  hybridization [10,11], resulting in slightly bent acetylene molecules. These studies also show that the existence of isolated three-fold sites alone is not a sufficient condition for the cyclotrimerization of acetylene, but it is suggested that the catalytically effective surface ensemble corresponds to three  $C_2H_2$  molecules adsorbed on three-fold sites around a given Pd atom [8,9]. This geometrical requirement is perfectly fulfilled for an ensemble of seven Pd atoms of the Pd(111) surface [5,12] and it is this argument, which explains the structure sensitivity of the cyclotrimerization reaction.

The formation of benzene on large palladium particles of typically thousands of atoms is very similar to the analogous low-index single-crystal results, with desorption of benzene at 230 and 530 K [13]. In contrast, small particles of typically hundreds of atoms are less selective for the cyclotrimerization and catalyze butadiene and butene as additional products [14]. Finally, it is interesting to note that the polymerization of acetylene over supported Pd particles reveals a direct correspondence between reactivities observed on model systems and the behavior of industrial catalysts under working conditions [14].

Here, we report a study of the acetylene polymerization on supported Pd atoms [15], on supported size-selected  $Pd_n$  clusters ( $2 \leq n \leq 30$ ) [16] and on size-distributed supported transition metal clusters ( $x < 50$ ) and we analyze the possibility to tune the selectivity of a reaction by changing the number of atoms per size-selected cluster or by changing the elemental composition.

## 2. Methods

### 2.1. Experimental

The transition metal clusters have been produced by a recently developed high-frequency laser evaporation source, ionized, then guided by ion optics through differentially pumped vacuum chambers and size-selected by a quadrupole mass spectrometer [17]. Most of the total deposition energy, being smaller than the binding energies of the investigated clusters [18], is rapidly dissipated via the solid surface [19]. Therefore, under these conditions the clusters soft-land (that is, without fragmentation) on the substrate [17,19,20]. Softlanding of the clusters on the oxide supports is also suggested by first principle calculations where  $Au_8$  is deposited on various MgO surfaces showing that the cluster's structure is only slightly distorted in comparison to the gas phase [21]. The fact that clusters indeed maintain their identity upon deposition is also shown experimentally [22]. Deposition of less than 1% of a monolayer (ML) of clusters ( $1 \text{ ML} = 2.2 \times 10^{15}$  clusters/cm<sup>2</sup>) at a substrate temperature of 90 K assures isolated supported clusters pinned on the defect

sites of the support [22]. The support is prepared in situ by epitaxially growing thin MgO(100) films on a Mo(100) surface [23]. These films show bulk-like properties [24]. Small amounts of defects like steps, kinks [25,26] and F-centres [21,27] are detected by the desorption behavior of small molecules.

To obtain identical conditions for the study of the polymerization on different Pd cluster sizes or on different transition metal clusters we first exposed, using a calibrated molecular beam doser, the prepared model catalysts at 90 K to an average of 1 Langmuir (L) acetylene, corresponding to saturation coverage.<sup>1</sup> In a temperature programmed reaction (TPR) catalytically formed benzene (C<sub>6</sub>H<sub>6</sub>), butadiene (C<sub>4</sub>H<sub>6</sub>) and butene (C<sub>4</sub>H<sub>8</sub>) molecules are detected by mass spectrometry (unambiguously characterized by their fragmentation patterns) and monitored as function of temperature.

## 2.2. Computational

The theoretical calculations have been carried out with the help of density functional theory (DFT) using either the gradient-corrected Becke's exchange functional [28] in combination with Perdew's correlation functional [29] (BP functional) or the Becke3 functional for exchange [30] and the Lee–Yang–Parr functional for correlation [31] (B3LYP functional). For further details about the computational aspects see for instance [15,32]. The MgO(001) surface has been represented by cluster models [33], an approach which has been found to reproduce in a sufficiently accurate way the electronic structure and the binding properties of surface complexes. Due to the highly ionic nature of MgO, the truncation of the lattice in cluster calculations implies the use of an external field to represent the long-range Coulomb potential. The model clusters considered have been embedded in arrays of point charges (PC =  $\pm 2e$ ) in order to reproduce the correct Madelung potential at the adsorption site under study [34]. The complete models, ions and PCs taken together, are electrically neutral. The positions of most substrate atoms and PCs were kept fixed at bulk-terminated values of MgO, with a measured bulk Mg–O distance of 2.104 Å [35]. Previ-

ous studies [36,37] have demonstrated that the use of PCs for embedding significantly affects the calculated adsorption properties when the positive PCs are nearest neighbors to the highly polarizable oxygen anions of the clusters. In that case, an artificial polarization of the oxygen anions at the cluster borders results; however, this artifact can be essentially eliminated by surrounding the anions with total ion model potentials (TIMPs) of Mg<sup>2+</sup> instead of positive PCs.

The positions of the supported Pd atom and of the surface ions closest to it and the structure of the adsorbed hydrocarbon molecules have been fully optimized using analytical energy gradients. The calculations have been performed with the GAUSSIAN98 [38] program package.

## 3. Results and discussions

### 3.1. Acetylene polymerization on supported Pd atoms

The smallest size-selected species being the monomer, we dedicate the first part to the study of the catalytic activity of Pd<sub>1</sub>/MgO(100) [39]. The TPR spectra of the different products of the polymerization of acetylene, obtained in a single pass heating cycle in vacuum, on supported palladium atoms and on the bare MgO films are shown in Fig. 1. As expected, the oxide support does not catalyze the polymerization reaction. However, as soon as palladium atoms are present, desorption of benzene is observed at 200 or 300 K, respectively. The reaction temperature is sensitively dependant on the film morphology [32]. We note that only the benzene is catalyzed, reflecting a selectivity of 100% for the cyclotrimerization reaction. In contrast to single-crystal studies, suggesting a minimum ensemble of seven Pd atoms for the reaction to occur [5,12], on MgO already a single Pd atom is sufficient to catalyze this reaction.

This surprising result was investigated theoretically by depositing a Pd atom onto different MgO sites represented by a cluster model [40]. First, it is interesting to note that on a single free Pd atom two C<sub>2</sub>H<sub>2</sub> molecules are slightly activated and transform into a C<sub>4</sub>H<sub>4</sub> intermediate with an energy gain of 3.9 eV [32]. The third acetylene molecule, however, is only weakly bound at a long distance of 2.6 Å and is practically

<sup>1</sup> Under these conditions the clusters are saturated with C<sub>2</sub>H<sub>2</sub> as desorption of physisorbed C<sub>2</sub>H<sub>2</sub> from the MgO films is detected at around 150 K.

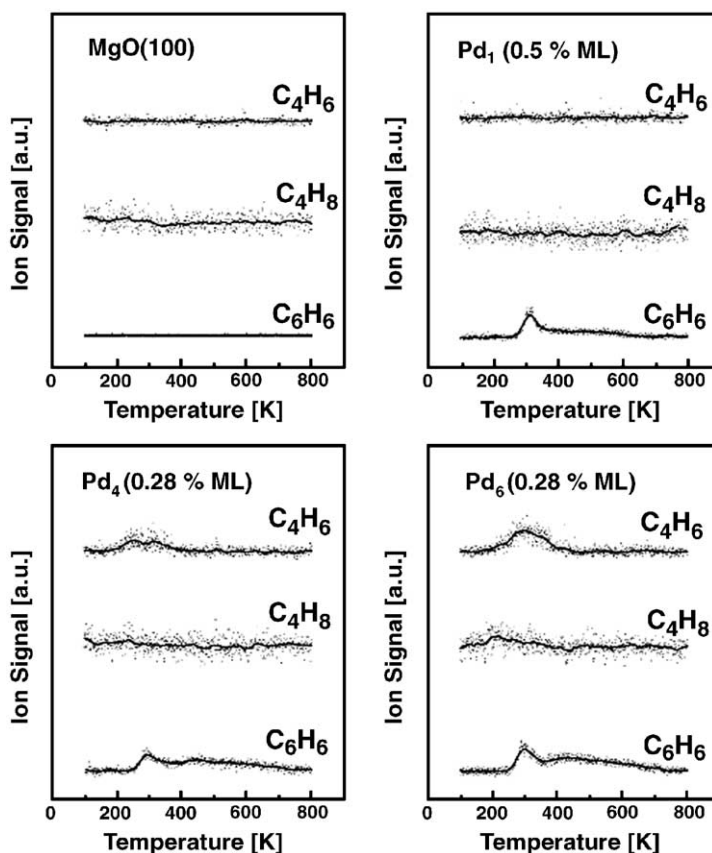


Fig. 1. TPR spectra of the catalytic formation of  $C_6H_6$ ,  $C_4H_8$ , and  $C_4H_6$  for Pd, Pd<sub>4</sub>, Pd<sub>6</sub>, Pd<sub>8</sub>, Pd<sub>13</sub>, Pd<sub>20</sub>, and Pd<sub>30</sub>. Note that clean MgO thin films do not catalyze the formation of these products. The relative ion intensities are corrected with the relative detection efficiencies of the experiment and scaled with the number of formed product molecules per cluster.

not activated; thus, cyclotrimerization does not occur. However, for negatively charged Pd atoms carrying a  $-0.3$  or  $-0.6$  net electronic charge, the structure of the  $C_4H_4$  intermediate is not altered, but the third acetylene molecule becomes more activated (e.g. the HCC angle decreases from  $177^\circ$  on neutral  $Pd(C_4H_4)$  to  $156^\circ$  on  $[Pd(C_4H_4)]^{-0.6}$ ), which enables formation of benzene. This suggests that the MgO substrate may increase the electron density on the supported Pd atoms. A Pd atom was then deposited on a five-coordinated oxygen ion on the MgO(100) terrace,  $O_{5c}$ . It was found that the  $Pd(C_4H_4)$  complex is indeed formed. The third acetylene molecule is however not bound to the  $Pd(C_4H_4)$  complex and the trimerization process does not occur. On an  $O_{5c}$  ion of the MgO(100) terrace the Pd atom is bound by approximately 1 eV

(DFT-B3LYP results [41]). This is not the most likely site to stabilize the Pd atoms on the MgO surface. In fact, upon deposition, the Pd atoms will diffuse on the surface until they are trapped at some defect site. The barrier for diffusion has been estimated to be approximately 0.5 eV. Several possible defect sites can bind a Pd atom more strongly.

On four-coordinated step or three-coordinated corner oxygen sites,  $O_{4c}$  and  $O_{3c}$ , respectively, the bonding is slightly larger than on the terrace, 1.2–1.5 eV and the Pd atom is more reactive. In fact, the formed  $Pd(C_4H_4)$  complex binds and activates the third acetylene molecule which has now an elongated C–C bond (1.304 Å) and a small HCC angle of  $142^\circ$ . The reason for this activation is an increased flow of electronic charge from the supported Pd atom to the

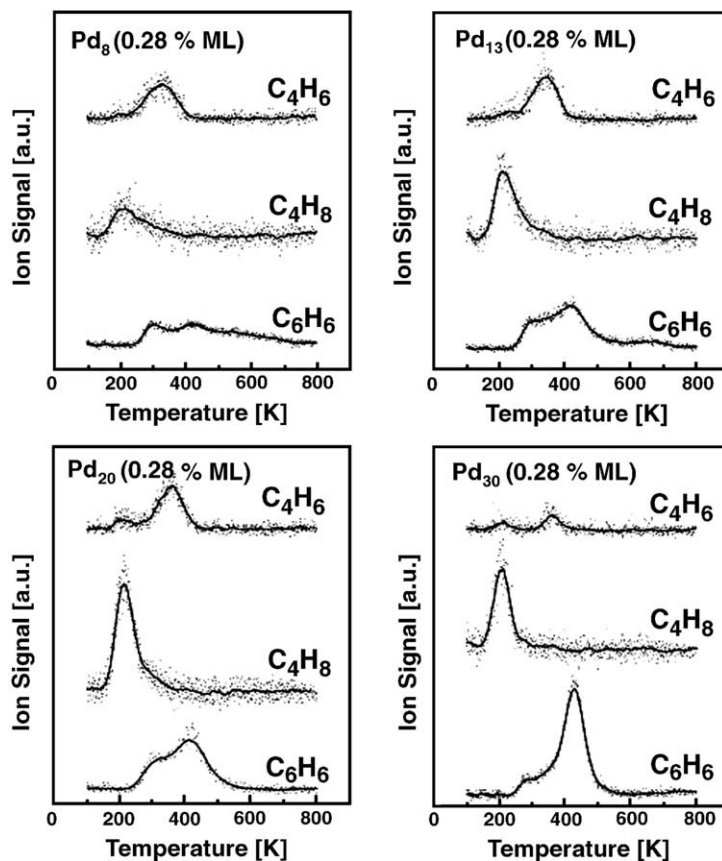


Fig. 1. (Continued).

adsorbed molecule. This is consistent with the higher basicity of the oxygen ions at low coordinated sites due to the lower Madelung potential at these sites [42]. Hence, the oxide support transforms the ‘inert’ free Pd atom into a more active species. However, on both O<sub>3c</sub> and O<sub>4c</sub> sites, the third C<sub>2</sub>H<sub>2</sub> molecule is only weakly bound to the Pd(C<sub>4</sub>H<sub>4</sub>) surface complex. This means that by raising the temperature, the third acetylene will desorb before reaction. Thus, Pd atoms adsorbed on O<sub>nc</sub> sites are not good models to explain the observed activity. This is consistent with the results of a recent experimental–theoretical study on the adsorption properties of CO on Pd<sub>1</sub>/MgO [41], which excludes the stabilization of Pd atoms at low-coordinated oxygen ions.

The experimental results can be rationalized in terms of Pd atoms, which are stabilized on oxygen vacancies, the F-centres, in neutral or charged states,

F<sub>s</sub> or F<sub>s</sub><sup>+</sup>, respectively. These centres are characterized by the presence of two (F<sub>s</sub>) or one (F<sub>s</sub><sup>+</sup>) trapped electrons [43]. The interaction of a Pd atom with an F<sub>5c</sub>-centre on a MgO terrace is very strong, 3.4 eV, thus these centres likely bind Pd atoms. On F<sub>s</sub><sup>+</sup> centres binding energies of approximately 2 eV have been computed [41]. The presence of trapped electrons at the defect site results in a more efficient activation of the supported Pd atom. In fact, the complex (C<sub>4</sub>H<sub>4</sub>)(C<sub>2</sub>H<sub>2</sub>)/Pd<sub>1</sub>/F<sub>5c</sub> shows a large distortion and a strong interaction of the third C<sub>2</sub>H<sub>2</sub> molecule. Thus, F and F<sup>+</sup> act as basic sites on the MgO surface and turn the inactive Pd atom into an active catalyst. Notice that the supported Pd atoms on defect sites not only activate the cyclization reaction, but also favour benzene desorption, as benzene is not bound to the (C<sub>6</sub>H<sub>6</sub>)/Pd<sub>1</sub>/F<sub>s</sub> complex due to the Pauli repulsion of the closed shell electronic structure of the

product molecule with the electronic states of the Pd atom.

The F-centres at the surface of MgO can be located at various sites, terraces, steps and edges, kinks and corners [43]. Therefore, a more accurate discrimination of the sites involved is desirable. To this end, we have computed the energy changes and the reaction barriers involved in the cyclization reaction for six different kinds of oxygen vacancies,  $F_{5c}$ ,  $F_{4c}$ ,  $F_{3c}$  and the corresponding paramagnetic charged centres  $F_{5c}^+$ ,  $F_{4c}^+$ ,  $F_{3c}^+$ . Here, we report for brevity only the reaction path for the  $F_{5c}$ -centre obtained at the DFT-BP level, Fig. 2. This is also the centre, which gives rise to the lowest barriers and to the most plausible reaction path. The first barrier in the reaction is that for the cycloaddition of two acetylene molecules,  $\text{Pd} + 2\text{C}_2\text{H}_2 \rightarrow \text{Pd}(\text{C}_4\text{H}_4)$  and is of only 0.48 eV, Fig. 2. The formation of the  $\text{C}_4\text{H}_4$  intermediate is thermodynamically favourable by 0.82 eV. On  $(\text{C}_4\text{H}_4)/\text{Pd}_1/\text{F}_{5c}$  the addition of the third acetylene molecule is exothermic by 1.17 eV, leading to a very stable  $(\text{C}_4\text{H}_4)(\text{C}_2\text{H}_2)/\text{Pd}_1/\text{F}_{5c}$  intermediate. To transform this intermediate into benzene one has to overcome a barrier of 0.98 eV, Fig. 2. Once formed,  $\text{C}_6\text{H}_6$  is so weakly bound to the supported Pd atom that it desorbs immediately. Thus, the reaction on  $\text{Pd}_1/\text{F}_{5c}$  is rate limited in the step of conversion of  $(\text{C}_4\text{H}_4)(\text{C}_2\text{H}_2)$

into  $\text{C}_6\text{H}_6$ . This is different from the  $\text{Pd}(111)$  surface, where the rate-determining step for the reaction is benzene desorption. The calculations are consistent with the experimental data. In fact, on  $\text{Pd}_1/\text{F}_{5c}$  the computed barrier of 0.98 eV corresponds to a desorption temperature of  $\approx 300$  K, as experimentally observed, Fig. 1. On  $\text{Pd}(111)$  surfaces, the bonding of benzene is estimated to be  $\approx 1.9$  eV (from a BP calculation on a  $\text{Pd}_6/(\text{C}_6\text{H}_6)$  cluster). This binding is consistent with the observed desorption temperature of  $\approx 500$  K [5].

The calculations rule out the F-centres at low-coordinated sites as the active centres. Pd on  $F_{4c}^{(0,+)}$  and  $F_{4c}^{(0,+)}$  centres, in fact, gives rise to energy barriers much too high to be reconciled with the observed desorption temperature. However, the calculations are not able to discriminate between the activity of neutral  $F_{5c}$  and charged  $F_{5c}^+$ -centres, as the barriers involved are of similar magnitudes.

### 3.2. Acetylene polymerization on supported size-selected Pd clusters

The TPR spectra of the different products of the polymerization of acetylene on small supported, monodispersed palladium clusters are shown in Fig. 1. Striking atom-by-atom size-dependent reactivities and selectivities are observed. Only the three

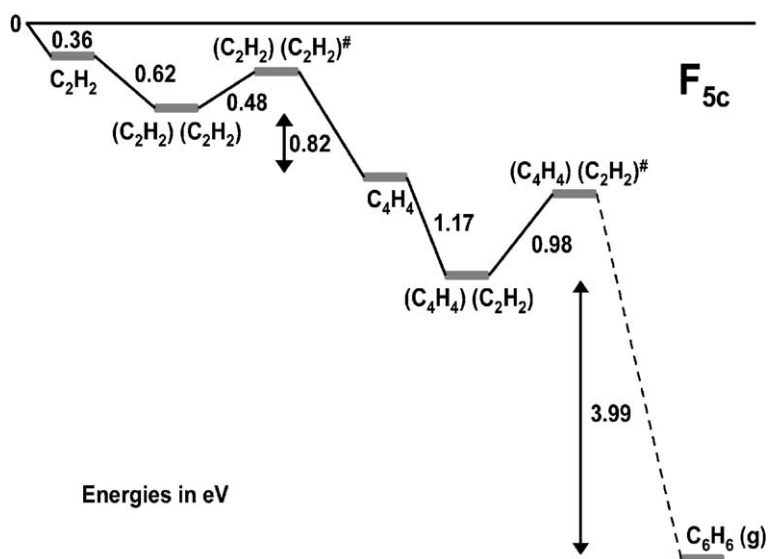


Fig. 2. Energy profile for the cyclization reaction of acetylene to benzene occurring on a Pd atom supported on a  $F_{5c}$ -centre,  $\text{Pd}_1/\text{F}_{5c}$  (DFT-BP results).

reaction products  $C_6H_6$ ,  $C_4H_8$ , and  $C_4H_6$  are detected. Remarkably, no  $C_3H_n$ ,  $C_5H_n$  and  $C_8H_n$  are formed, indicating the absence of C–C bond scission as already observed on Pd single crystals [7] and Pd particles [14]. Up to Pd<sub>3</sub>, only benzene is catalyzed reflecting a high selectivity for the cyclotrimerization of acetylene. Pd<sub>*n*</sub> ( $4 \leq n \leq 6$ ) clusters reveal a second reaction channel by catalyzing in addition the formation of  $C_4H_6$ , which desorbs at around 300 K. The third reaction product,  $C_4H_8$ , desorbing at a rather low temperature of 200 K, is clearly observed for Pd<sub>8</sub>. For this cluster size the abundance of the three reaction products is similar. For even larger clusters ( $13 \leq n \leq 30$ ) the formation of  $C_6H_6$  is increasing with cluster size, whereas the conversion of acetylene into  $C_4H_8$  reaches a maximum for Pd<sub>20</sub>. Note that Pd<sub>30</sub> selectively suppresses the formation of  $C_4H_6$ . (The peak in the TPR spectrum of  $C_4H_6$  at 200 K is part of the fragmentation pattern of  $C_4H_8$ .) For Pd<sub>20</sub> the experiments were repeated in the presence of D<sub>216</sub>; D<sub>2</sub> was exposed prior and after C<sub>2</sub>H<sub>2</sub>. The results clearly indicate that no product containing deuterium is formed. Consequently D<sub>2</sub> is not involved in the polymerization reaction. However, the presence of D<sub>2</sub> opens a new reaction channel, the hydrogenation of acetylene. In addition, D<sub>2</sub> blocks the active sites on the palladium clusters for the polymerization, as the formation of the products is slightly reduced when exposing D<sub>2</sub> prior to C<sub>2</sub>H<sub>2</sub>. On Pd(1 1 1), pre-dosing with H<sub>2</sub> completely suppresses the cyclotrimerization but enhances the hydrogenation of acetylene to form ethylene [4].

The relative ion intensities of the products in the TPR spectra scale with the product formation by the model catalysts.<sup>2</sup> By integrating the total area of the TPR spectra shown in Fig. 1, the number of catalytically produced benzene, butadiene and butene molecules per cluster is obtained and illustrated in Fig. 3a. Fig. 3b shows the selectivities *S* for the formation of the products P<sub>1</sub> ( $C_6H_6$ ), P<sub>2</sub> ( $C_4H_6$ ), and P<sub>3</sub> ( $C_4H_8$ ) for different cluster sizes calculated from, e.g.:

$$S(P_1) = \left( \frac{\text{number of } P_1 \text{ per cluster}}{\text{number of } \Sigma P_n \text{ per cluster}} \right) \times 100 (\%)$$

<sup>2</sup> The mass spectrometer was calibrated for the three species using a flow-calibrated molecular beam doser and relative detection efficiencies of the three measured masses (78 for benzene, 56 for  $C_4H_8$ , and 54 for  $C_4H_6$ ) were obtained.

The striking atom-by-atom size-dependent selectivity for the polymerization of acetylene is summarized as follows:  $C_6H_6$  is catalyzed with a selectivity of 100% on cluster sizes up to Pd<sub>3</sub>. The selectivity for  $C_4H_6$  reaches a maximum for Pd<sub>6</sub> (~30%) and the production of  $C_4H_8$  is most efficient (~40%) for Pd<sub>20–25</sub>. If we assume stoichiometric reactions, as indicated in Fig. 3c, and estimate the relative number of reacted C<sub>2</sub>H<sub>2</sub> from Fig. 3a, we observe a proportional increase of acetylene with the number of Pd atoms per cluster up to Pd<sub>13</sub>. Surprisingly, at this cluster size the surface-to-bulk ratio as well as the coordination number of Pd in the cluster is changing as at this size one Pd atom sits completely in the cluster. In addition, according to the three stoichiometric chemical reactions, each reaction requires minimum number of Pd atoms, which are 3, 4, and 6. The experimental results are surprisingly consistent, that is  $C_4H_6$  is formed for Pd<sub>*n*</sub> with  $n \geq 4$  and  $C_4H_8$  for cluster sizes with  $n \geq 6$ .

Analyzing the products formed on small size-selected Pd<sub>*n*</sub> ( $1 \leq n \leq 30$ ) clusters deposited on MgO(100) thin films indicates that the surface intermediate  $C_4H_4$  is being produced efficiently on all cluster sizes. Thus, at least two acetylene molecules are adsorbed in a  $\pi$ -bonded configuration at the initial stage of the reaction [32]. The observed size-dependent selectivity may then be understood by regarding the influence of the cluster size to steer the reaction either towards the cyclotrimerization to form  $C_6H_6$  or towards a direct hydrogen transfer from adsorbed C<sub>2</sub>H<sub>2</sub> to the  $C_4H_4$  intermediate to catalyze the formation of  $C_4H_6$  or  $C_4H_8$ , respectively. Direct hydrogen transfer is shown to occur as in an independent experiment coadsorption of D<sub>2</sub> does not result in product molecules containing deuterium atoms, the presence of D<sub>2</sub>, however, slightly decreases the reactivity of the model catalysts. Cyclotrimerization is generally observed when a third acetylene molecule is adsorbed in a  $\pi$ -bonded configuration, which results in a change from sp-hybridization towards a sp<sup>2</sup>-hybridization [6]. This bonding configuration leads to a weak activation of the C–H bond, in analogy to ethylene [44]. The hydrogenation of the Pd<sub>*n*</sub>( $C_4H_4$ ) metallocycle, on the other hand, is favored by the adsorption of di- $\sigma/\pi$ -bonded acetylene to three Pd-atoms, effecting a more efficient activation of the C–H bond, in analogy to ethylene [44].

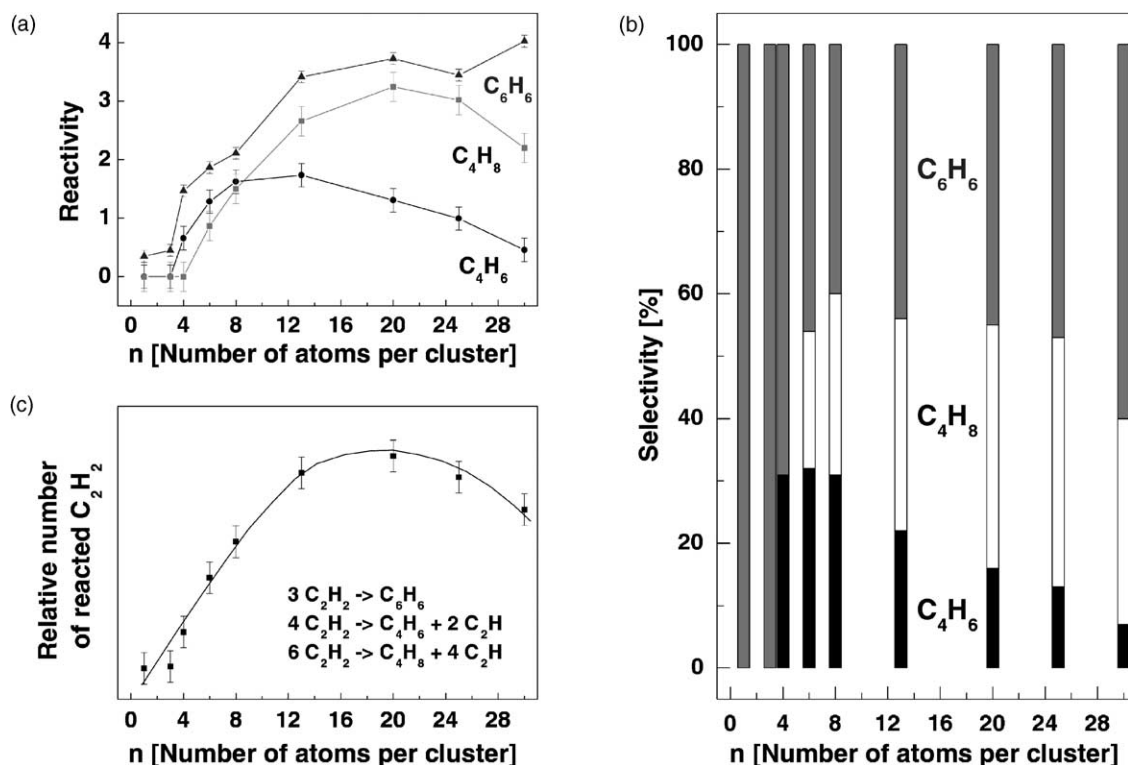


Fig. 3. (a) Cluster size dependent reactivity expressed in the relative number per cluster of formed product molecules, C<sub>6</sub>H<sub>6</sub>, C<sub>4</sub>H<sub>8</sub>, and C<sub>4</sub>H<sub>6</sub>. Maximal reactivity for the formation of C<sub>4</sub>H<sub>6</sub> for cluster sizes around Pd<sub>10</sub>, for the formation of C<sub>4</sub>H<sub>8</sub> for cluster sizes around Pd<sub>20</sub>. The formation of C<sub>6</sub>H<sub>6</sub> is increasing with size; (b) size dependent selectivity in % for the polymerization of acetylene (see text). Pd<sub>1–3</sub> show 100% selectivity for the cyclotrimerization, whereas the selectivity for the hydrogenation of the intermediate, C<sub>4</sub>H<sub>4</sub> to C<sub>4</sub>H<sub>6</sub> (30%) and C<sub>4</sub>H<sub>8</sub> (~40%) is maximal for Pd<sub>6</sub> and Pd<sub>20–25</sub>, respectively; (c) relative number of reacted C<sub>2</sub>H<sub>2</sub> as a function of cluster size. The values are obtained from (a) and by using the stoichiometric reactions shown in the figure.

For Pd atoms adsorbed on defect sites the Pd(C<sub>4</sub>H<sub>4</sub>) intermediate is formed with an energy gain of around 2 eV (Fig. 2). A third adsorbed C<sub>2</sub>H<sub>2</sub> molecule is purely  $\pi$ -bonded (Fig. 4a) and the activated acetylene molecule reacts with the intermediate to form benzene with a total exothermicity of about 4 eV. The weakly bound C<sub>6</sub>H<sub>6</sub> (0.3 eV) then desorbs at low temperature from the model catalyst [32]. A second reaction channel, the formation of butadiene, C<sub>4</sub>H<sub>6</sub>, opens for Pd<sub>4</sub>. This channel reveals highest selectivity for Pd<sub>6</sub>, in this case a third C<sub>2</sub>H<sub>2</sub> molecule can bind in a di- $\sigma$ / $\pi$ -bond configuration to three Pd atoms (as shown in Fig. 4b). The charge transfer from the substrate to the cluster further enhances the activation of the C–H bonds. For even larger cluster sizes the adsorption of two di- $\sigma$ / $\pi$ -bonded C<sub>2</sub>H<sub>2</sub> molecules be-

comes possible (Fig. 4c) and opens up the third reaction path, the formation of C<sub>4</sub>H<sub>8</sub>. In our experiments this is clearly observed for Pd<sub>8</sub>. Purely geometrical arguments (possible adsorption of two di- $\sigma$ / $\pi$ -bonded C<sub>2</sub>H<sub>2</sub> molecules close to the C<sub>4</sub>H<sub>4</sub> intermediate) suggest that this third channel is more pronounced for the larger clusters, and indeed our results show maximal C<sub>4</sub>H<sub>8</sub> formation for cluster sizes of 20–25 Pd atoms. For the largest clusters of the measured range, e.g. Pd<sub>30</sub>, the increased number of metal–metal bonds and the concomitant delocalization of the charge transferred from the substrate to the cluster results in less charge density available for the activation of the C–H bond [45]. Consequently, the cyclotrimerization becomes again more efficient than the hydrogenation of the C<sub>4</sub>H<sub>4</sub> intermediate. Going to even larger particles



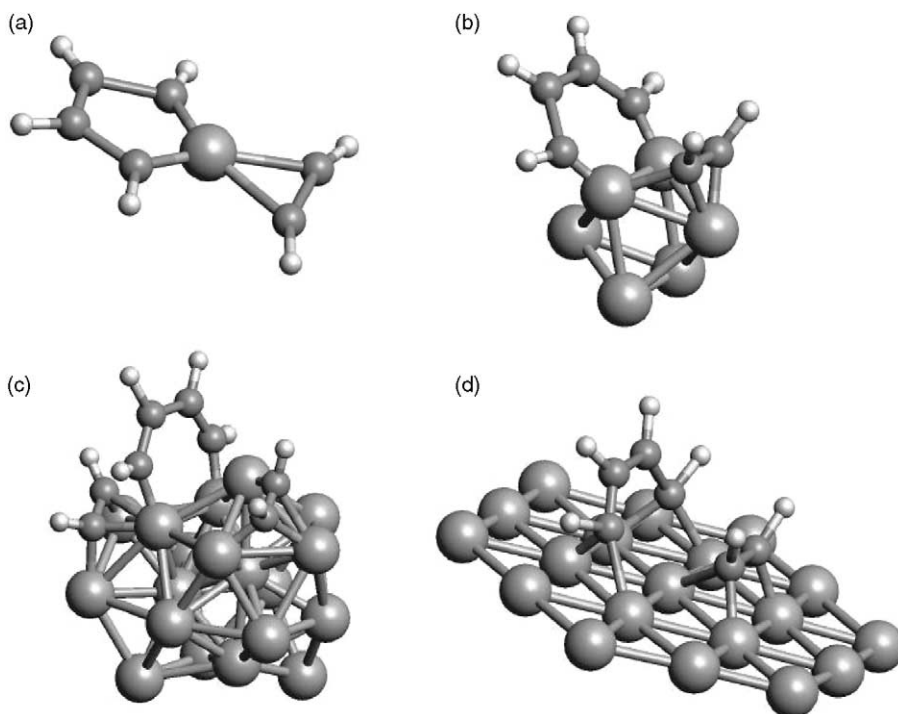


Fig. 4. Proposed structures of the complexes. (a)  $\text{Pd}(\text{C}_4\text{H}_4)^{-0.6}(\text{C}_2\text{H}_2)$   $\pi$ -bonded [32]; (b)  $\text{Pd}_6(\text{C}_4\text{H}_4)(\text{C}_2\text{H}_2)$  di- $\sigma/\pi$ -bonded,  $\text{Pd}_6$  structure taken from [15]; (c)  $\text{Pd}_{20}(\text{C}_4\text{H}_4)_2(\text{C}_2\text{H}_2)$  di- $\sigma/\pi$ -bonded,  $\text{Pd}_{20}$  structure (Morse cluster) taken from [46]; and (d)  $\text{Pd}(111)(\text{C}_4\text{H}_4)(\text{C}_2\text{H}_2)$  di- $\sigma/\pi$ -bonded [6]. In this schematic representation the cluster structures were obtained from existing calculations. For  $\text{Pd}_6$  and  $\text{Pd}_{20}$ , the adsorption configuration of  $\text{C}_2\text{H}_2$  and  $\text{C}_4\text{H}_4$  are taken in analogy to the surface structures [6].

or to  $\text{Pd}(111)$  single crystals the cyclotrimerization to benzene is selectively catalyzed (Fig. 4d).

### 3.3. Acetylene polymerization on supported transition metal clusters

On single crystals the cyclotrimerization of acetylene is rather specific to palladium surfaces; with the exception of  $\text{Cu}(110)$  and  $\text{Ni}(111)$ , the latter with low efficiency. No other metal surface has been reported as being active towards the formation of benzene [1]. For supported transition metal clusters, an exception has to be added: cobalt. In Fig. 5, the TPR spectra of different products of the polymerization of acetylene on small size-distributed, supported transition metal clusters ( $n < 50$ ) are shown. As already discussed above, size-selected clusters catalyze the polymerization of acetylene with the product molecules, benzene, butene, and butadiene. The benzene desorbs at around 240 and 400 K, the butene

at around 250 K and the butadiene at around 330 K. This palladium catalyst is the most efficient supported transition metal clusters catalyst to produce benzene. As noted above for single-crystal studies, the second most active catalyst consists of copper, where benzene desorbs at around 320 K. On the supported copper clusters, only one other product molecule, butadiene, is detected. It desorbs at around 330 K with efficiencies similar to the palladium catalyst. As no butene is produced, the selectivities for  $\text{C}_6\text{H}_6$  and  $\text{C}_4\text{H}_6$  are larger than on palladium catalysts. To increase the selectivity for  $\text{C}_6\text{H}_8$ , the use of supported nickel clusters is favorable. Indeed, on supported nickel catalysts, no butadiene is produced and desorption of benzene is drastically reduced. Desorption of butene is observed at around 250 K with a similar efficiency as for supported palladium catalyst. On cobalt catalysts, the selectivity for  $\text{C}_6\text{H}_6$  is almost 100%, as no butadiene and butene are produced, but the catalytic activity of these cobalt clusters is very low in com-

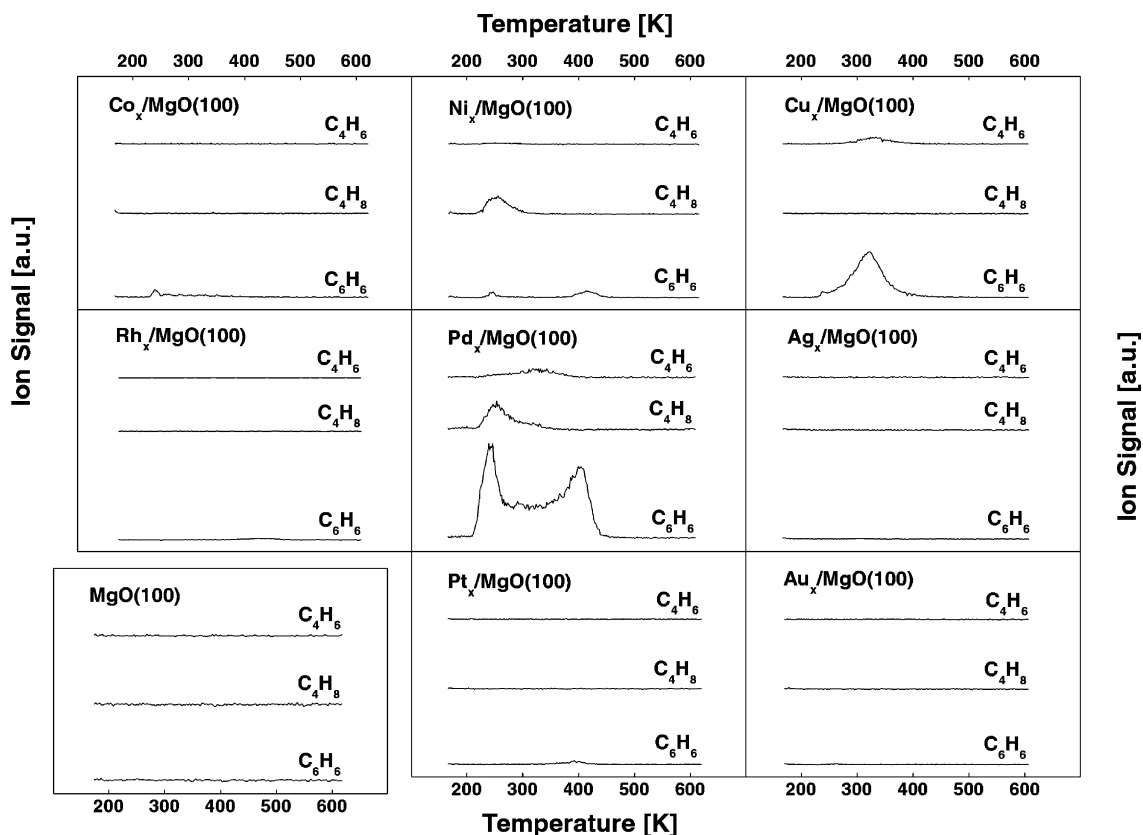


Fig. 5. TPR spectra of the catalytic formation of  $C_6H_6$ ,  $C_4H_8$ , and  $C_4H_6$  for  $Co_x/MgO(100)$ ,  $Ni_x/MgO(100)$ ,  $Cu_x/MgO(100)$ ,  $Rh_x/MgO(100)$ ,  $Pd_x/MgO(100)$ ,  $Ag_x/MgO(100)$ ,  $Pt_x/MgO(100)$  and  $Au_x/MgO(100)$  catalysts. The cluster densities of nanocatalysts are 0.88 ML. The relative ion intensities are corrected with the relative detection efficiencies of the experiment and scale with the number of formed product molecules per cluster.

parison with palladium or copper clusters. Finally,  $Rh_x/MgO(100)$ ,  $Ag_x/MgO(100)$ ,  $Pt_x/MgO(100)$  and  $Au_x/MgO(100)$  catalysts are inactive towards the formation of benzene from acetylene.

#### 4. Conclusion

The properties of nanocatalysts are distinctly different than those of conventional catalysts. In the case of palladium, already single atoms, dimers, and trimers are active and highly selective for the cyclotrimerization of acetylene. The reason for this behavior is the  $\pi$ -bonding of acetylene and a charge transfer from the substrate to the atom/clusters. In addition, for these nanoscale palladium catalysts the

rate-determining step is the formation of benzene from the  $Pd(C_4H_4)C_2H_2$  complex. For larger  $Pd_n$  ( $1 < n < 30$ ) the selectivity of the polymerization can be tuned atom-by-atom, with maximum selectivities for the formation of butadiene or butene for  $Pd_6$  or  $Pd_{20-25}$ , respectively. For supported transition metal clusters cobalt turns reactive in contrast to the bulk analogue and is extremely selective for the cyclotrimerization reaction. Thus, nanocatalysis opens new avenues to tune activities and selectivities of catalytic processes.

#### Acknowledgements

The experimental work was supported by the Swiss National Science Foundation and by the 'Deutsche

Forschungsgemeinschaft'. The theoretical work was supported in part by the Italian INFM through the PRA-ISADORA project. K. Judai acknowledges a fellowship from the Humboldt-Foundation. S. Abbet acknowledges a fellowship from the Swiss National Science Foundation. We also thank the referee for his contribution.

## References

- [1] R.M. Lambert, R.M. Ormerod, in: R.J. Madix (Ed.), *Surface Reactions*, vol. 34, Springer, Berlin, 1994, pp. 89–144.
- [2] T.M. Gentle, E.L. Muettterties, *J. Phys. Chem.* 87 (1983) 2469–2472.
- [3] T.G. Rucker, M.A. Logan, T.M. Gentle, E.L. Muettterties, G.A. Somorjai, *J. Phys. Chem.* 90 (1986) 2703–2708.
- [4] W.T. Tysoe, G.L. Nyberg, R.M.J. Lambert, *J. Chem. Soc., Chem. Commun.* (1983) 623–625.
- [5] R.M. Ormerod, R.M. Lambert, *J. Phys. Chem.* 96 (1992) 8111–8116.
- [6] G. Pacchioni, R.M. Lambert, *Surf. Sci.* 304 (1994) 208–222.
- [7] C.H. Patterson, R.M. Lambert, *J. Phys. Chem.* 92 (1988) 1266–1270.
- [8] H. Hoffmann, F. Zaera, R.M. Ormerod, R.M. Lambert, J.M. Yao, D.K. Saldin, L.P. Wang, D.W. Bennett, W.T. Tysoe, *Surf. Sci.* 268 (1992) 1–10.
- [9] J.A. Gates, L.L. Kesmodel, *J. Chem. Phys.* 76 (1982) 4281–4286.
- [10] P.Y. Timbrell, A.J. Gellman, R.M. Lambert, R.F. Willis, *Surf. Sci.* 206 (1988) 339–347.
- [11] H. Sellers, *J. Phys. Chem.* 94 (1990) 8329–8333.
- [12] C.J. Baddeley, M. Tikhov, C. Hardacre, J.R. Lomas, R.M. Lambert, *J. Phys. Chem.* 100 (1996) 2189–2194.
- [13] P.M. Holmblad, D.R. Rainer, D.W. Goodman, *J. Phys. Chem. B* 101 (1997) 8883–8886.
- [14] R.M. Ormerod, R.M. Lambert, *J. Chem. Soc., Chem. Commun.* (1990) 1421.
- [15] S. Abbet, A. Sanchez, U. Heiz, W.-D. Schneider, A.M. Ferrari, G. Pacchioni, N. Roesch, *Surf. Sci.* 454/456 (2000) 984–989.
- [16] S. Abbet, A. Sanchez, U. Heiz, W.-D. Schneider, *J. Catal.* 198 (2001) 122–127.
- [17] U. Heiz, F. Vanolli, L. Trento, W.-D. Schneider, *Rev. Sci. Instrum.* 68 (1997) 1986.
- [18] U. Heiz, W.-D. Schneider, *J. Phys. D: Appl. Phys.* 33 (2000) R85–R102.
- [19] H.-P. Cheng, U. Landman, *J. Phys. Chem.* 98 (1994) 3527.
- [20] K. Bromann, C. Felix, H. Brune, W. Harbich, R. Monot, J. Buttet, K. Kern, *Science* 274 (1996) 956–958.
- [21] A. Sanchez, S. Abbet, U. Heiz, W.-D. Schneider, H. Haekkinen, R.N. Barnett, U. Landman, *J. Phys. Chem. A* 103 (1999) 9573–9578.
- [22] S. Abbet, K. Judai, L. Klinger, U. Heiz, *Pure Appl. Chem.* 74 (9) (2002) 1527.
- [23] M.C. Wu, J.S. Corneille, C.A. Estrada, J.-W. He, D.W. Goodman, *Chem. Phys. Lett.* 182 (5) (1991) 472.
- [24] M.-H. Schaffner, F. Patthey, W.-D. Schneider, L.G.M. Pettersson, *Surf. Sci.* 450 (1998) 402–404.
- [25] R. Soave, G. Pacchioni, *Chem. Phys. Lett.* 320 (2000) 345–351.
- [26] C. Di Valentin, G. Pacchioni, M. Chiesa, E. Giamello, S. Abbet, U. Heiz, *J. Phys. Chem. B* 106 (7) (2002) 1637.
- [27] C. Di Valentin, G. Pacchioni, S. Abbet, U. Heiz, *J. Chem. Phys. B*, submitted for publication.
- [28] A.D. Becke, *Phys. Rev. A* 38 (1988) 3098.
- [29] J.P. Perdew, *Phys. Rev. B* 33 (1986) 8822.
- [30] A.D. Becke, *J. Chem. Phys.* 98 (1993) 5648.
- [31] C. Lee, W. Yang, R.G. Parr, *Phys. Rev. B* 37 (1988) 785.
- [32] S. Abbet, A. Sanchez, U. Heiz, W.-D. Schneider, A.M. Ferrari, G. Pacchioni, N.J. Roesch, *Am. Chem. Soc.* 122 (2000) 3453–3457.
- [33] G. Pacchioni, P.S. Bagus, F. Parmigiani (Eds.), *Cluster Models for Surface and Bulk Phenomena*, vol. 283, Plenum Press, New York, 1992.
- [34] G. Pacchioni, A.M. Ferrari, A.M. Marquez, F. Illas, *J. Comp. Chem.* 18 (1997) 617.
- [35] R.W.G. Wyckoff, *Crystal Structures*, second ed., Interscience, New York, 1965.
- [36] I.V. Yudanov, S. Vent, K. Neyman, G. Pacchioni, N. Rösch, *Chem. Phys. Lett.* 275 (1997) 245–252.
- [37] M.A. Nygren, L.G.M. Pettersson, Z. Barandiaran, L.J. Seijo, *Chem. Phys.* 100 (1994) 2010.
- [38] M.J. Frisch, et al., *Gaussian98*, Gaussian Inc., Pittsburgh, PA, 1998.
- [39] S. Abbet, A.M. Ferrari, L. Giordano, G. Pacchioni, H. Hakkinen, U. Landman, U. Heiz, *Surf. Sci.* 514 (2002) 249.
- [40] A.M. Ferrari, L. Giordano, G. Pacchioni, S. Abbet, U. Heiz, *J. Phys. Chem B* 106 (12) (2002) 3173.
- [41] S. Abbet, E. Riedo, H. Brune, U. Heiz, A.M. Ferrari, L. Giordano, G. Pacchioni, *J. Am. Chem. Soc.* 123 (2001) 6172–6178.
- [42] G. Pacchioni, J.M. Ricart, F. Illas, *J. Am. Chem. Soc.* 116 (1994) 10152.
- [43] G. Pacchioni, P. Pescarmona, *Surf. Sci.* 412/413 (1998) 657–671.
- [44] A. Fahmi, R.A. van Santen, *J. Phys. Chem.* 100 (1996) 5676–5680.
- [45] S. Burkart, N. Blessing, G. Ganterför, *Phys. Rev. B* 60 (1999) 15639.
- [46] C. Roberts, R.L. Johnston, N.T. Wilson, *Theor. Chem. Acc.* 104 (2000) 123.
- [47] I.M. Abdelrehim, K. Pelhos, T.E. Madey, J. Eng Jr., J.G. Chen, *J. Mol. Catal. A* 131 (1998) 107–120.